Analysis of intermolecular interactions of n-perfluoroalkanes with circumcoronene using dispersion-corrected DFT calculations: Comparison with those of n-alkanes

Journal:	*Physical Chemistry Chemical Physics*
Manuscript ID	CP-ART-02-2023-000790.R1
Article Type:	Paper
Date Submitted by the Author:	19-Mar-2023
Complete List of Authors:	Kikkawa, Yoshihiro; National Institute of Advanced Industrial Science and Technology (AIST), Tsuzuki, Seiji; The University of Tokyo, Applied Physics; Yokohama National University, Institute of Advanced Sciences

ARTICLE

Analysis of intermolecular interactions of *n*-perfluoroalkanes with circumcoronene using dispersion-corrected DFT calculations: Comparison with those of *n*-alkanes

Received 00th January 20xx,
Accepted 00th January 20xx

DOI: 10.1039/x0xx00000x

Yoshihiro Kikkawa*[a] and Seiji Tsuzuki*[b]

Understanding the interactions between the adsorbate and substrate is critical in basic and advanced scientific fields, including the formation of well-organised nanoarchitectures via self-assembly on surfaces. In this study, the interactions of *n*-alkanes and *n*-perfluoroalkanes with circumcoronene were studied using dispersion-corrected density functional theory calculations as models of their adsorption on graphite. The interactions of *n*-perfluoroalkanes with circumcoronene were significantly weaker than those of the corresponding *n*-alkanes, e.g. the calculated adsorption energies of *n*-perfluorohexane and *n*-hexane were –9.05 and –13.06 kcal mol^{-1}, respectively. The dispersion interactions were the major source of attraction between circumcoronene and the adsorbed molecules. Larger steric repulsion of *n*-perfluoroalkanes compared to those of *n*-alkanes increased their equilibrium distances from circumcoronene and decreased the dispersion interactions, resulting in weaker interactions. The interactions between two adsorbed *n*-perfluorohexane molecules and those of *n*-hexane molecules were –2.96 and –2.98 kcal mol^{-1}, respectively, which are not negligible in the stabilisation of adsorbed molecules. The geometries of adsorbed *n*-perfluoroalkane dimers revealed that the equilibrium distance between two *n*-perfluoroalkane molecules did not match the width of the six-membered rings in circumcoronene, in contrast to that between *n*-alkanes. The lattice mismatch also destabilised the adsorbed *n*-perfluoroalkane dimers. The difference in the adsorption energy between flat-on and edge-on orientations of *n*-perfluorohexane was smaller than that of corresponding *n*-hexane.

Introduction

Molecular adsorption on surfaces is critical not only in the basic scientific fields, but also in various applications, such as friction, lubrication, and self-assembled coating.[1] The adsorption energies (E_{ad}) of molecules on surfaces are actively studied owing to their significance in these research fields. The E_{ad} values of various molecules on graphite surfaces have been studied using temperature-programmed desorption (TPD) measurements.[2] Tait et al.[2e] reported a linear relationship between the desorption energies of short-chain *n*-alkanes ($N \leq 10$, where N is number of carbon atoms) on a graphene surface and the alkyl chain length. Paserba and Gellman[2a–c] measured the desorption energies of *n*-alkanes with numerous chain lengths (N = 5–60).

Molecular adsorption on surfaces is also crucial in the formation of nanostructures via self-assembly on surfaces, which exhibits considerable potential for application in the fields of nanoelectronics, molecular devices, lithography masks, etc.[3] Various intermolecular interactions, such as hydrogen bonding[4], metal coordination[5], halogen bonding[6] and dispersion forces[7] are exploited in self-assembly. On the highly ordered pyrolytic graphite (HOPG) surface, the alkyl chains are critical in enhancing the stabilities of the adsorbed molecules. The interactions of the alkyl groups with the surface are important in the formation of self-assemblies on HOPG.

Various theoretical studies regarding alkane adsorption on graphene have been reported.[8,9] Thierfelder et al.[9a] reported the interaction energies between methane and graphene using van der Waals density functional (vdW-DF), dispersion-corrected density functional theory (DFT), and second-order Møller-Plesset perturbation theory (MP2) level calculations of the interaction energy between methane and coronene. Londero et al.[9b] determined the interaction energies of *n*-alkanes (N = 1–10) on graphene using vdW-DFT calculations, and Kamiya and Okada[9c] reported DFT calculations of the interaction energies of *n*-alkanes on carbon nanotubes using the local-density approximation functional. *n*-Alkane adsorption has also been studied using force field calculations and molecular dynamics simulations.[8a,b]

Fluoroalkane adsorption on surfaces is crucial in numerous research fields. Polytetrafluoroethylene and perfluoropolyether are used as fluorine-based lubricants, e.g. perfluoropolyether was used as a lubricant in hard disk drives.[10] Fluoroalkyl groups were also used in scanning tunnelling microscopy (STM) studies

---

[a] *National Institute of Advanced Industrial Science and Technology (AIST), Tsukuba Central 5, 1-1-1 Higashi, Tsukuba, Ibaraki 305-8565, Japan*
E-mail: y.kikkawa@aist.go.jp

[b] *Department of Applied Physics, The University of Tokyo, Tokyo 113-8656, Japan*
E-mail: tsuzuki.seiji@mail.u-tokyo.ac.jp

Electronic Supplementary Information (ESI) available: CCSD(T) calculations of the interaction energy potential of the C_6H_6-CF_4 complex and the adsorption energies of *n*-alkanes on coronene, and additional data calculated via DFT. See DOI: 10.1039/x0xx00000x of surface-adsorbed molecules. Partially fluorinated alkyl chains were used as chemical markers because the fluorinated moieties appear dark in STM images.[11]

Although numerous experimental and theoretical studies regarding alkane adsorption have been reported, few investigate perfluoroalkane adsorption. Alkyl groups stably adsorb on HOPG, but perfluoroalkyl groups do not.[11] Parker et al.[12] reported that *n*-dodecane preferentially adsorbs as a monolayer on graphite in a binary mixture with *n*-perfluorododecane. However, the differences in the interaction energies of *n*-alkanes and *n*-perfluoroalkanes with graphite and their origins are not well understood. Only one theoretical study with semiempirical quantum mechanical calculations of the interactions between *n*-perfluoroalkanes and graphene is reported.[13] The calculations suggest that the interactions of *n*-perfluoroalkanes are slightly stronger than those of *n*-alkanes, in contrast to the experimental results. Thus, perfluoroalkane adsorption on graphite is not well understood, and several critical fundamental issues remain unsettled: (1) The structures of adsorbed *n*-perfluoroalkanes on graphite; (2) the differences in the E_{ad} values of *n*-alkanes and *n*-perfluoroalkanes on graphite; (3) the origin of the attraction between graphite and adsorbed molecules (*n*-alkanes and *n*-perfluoroalkanes); (4) the origin of the differences in the E_{ad} values of *n*-alkanes and *n*-perfluoroalkanes; (5) the contributions of the interactions between the adsorbed molecules on graphite in their stabilisation. Although the significance of the interactions between adsorbed molecules in stable monolayer formation is reported, the magnitudes of these interactions are not well understood.

In this study, the stable structures of circumcoronene complexes with *n*-alkanes and *n*-perfluoroalkanes and their interaction energies were studied as models of adsorption on graphite. The intermolecular interaction energies obtained via coupled cluster calculations with single and double substitutions with noniterative triple excitations (CCSD(T))[14] using sufficiently large basis sets are generally consistent with the experimental values in the gas phase.[15] However, the computational time of a CCSD(T) calculation is proportional to the seventh power of the number of basis sets used in the calculation, and thus, the CCSD(T) calculations of circumcoronene complexes with *n*-alkanes and *n*-perfluoroalkanes are too computationally demanding. Therefore, we studied the geometries and interaction energies of the complexes using dispersion-corrected DFT calculations. The interaction energies were calculated using a combination of the functional and dispersion-correction methods, which can yield similar interaction energies to those obtained via the CCSD(T) calculations.[16] We also analysed the contributions of the electrostatic and dispersion interactions to elucidate the origin of the adsorbate-surface attraction.

Computational details

Gaussian 16 (Gaussian, Wallingford, CT, USA) was used in the DFT and *ab initio* calculations.[17] Geometry optimisations were performed at the B3LYP/6-31G* level[18] with Grimme's D3 dispersion correction[19] and basis set superposition error (BSSE) corrections[20] using the counterpoise method.[21] The geometry of optimised isolated circumcoronene was fixed, and only the geometries of the adsorbed molecules were optimised. The intermolecular interaction energy between circumcoronene and an adsorbate molecule (E_{int}) was calculated using the BSSE correction. E_{ad} was calculated as the sum of E_{int} and deformation energy (E_{def}), which is the increase in the energy of the adsorbed molecule due to the deformation associated with adsorption. E_{int} and E_{def} were calculated at the B3LYP/6-311G** level of theory with Grimme's D3 dispersion correction. E_{int} was evaluated at this level because the calculated interaction energy potentials of the benzene-methane and benzene-perfluoromethane complexes at this level were very close to the estimated CCSD(T)-level interaction energy potentials at the basis set limit ($E_{\mathrm{CCSD(T)(limit)}}$, Fig. S1). In addition, the calculated E_{ad} values of alkane adsorption on coronene at this level were close to the $E_{\mathrm{CCSD(T)(limit)}}$ values (Table S2). The details of the comparison with the CCSD(T) calculations are provided in the Supplementary Information. Computational methods for the evaluations of each energy term (electrostatic, induction etc.) are shown in ESI.

Results and discussion

The optimised geometries of the single *n*-alkanes adsorbed on circumcoronene are shown in Figs. 1A and S3. Their hydrogen atoms are located close to the centres of the six-membered rings of circumcoronene, and the symmetry planes of all-*trans* *n*-alkanes are almost parallel to the π-plane of circumcoronene. The distances between the carbon atoms of the adsorbed *n*-alkanes and the π-plane are approximately 3.5 Å.

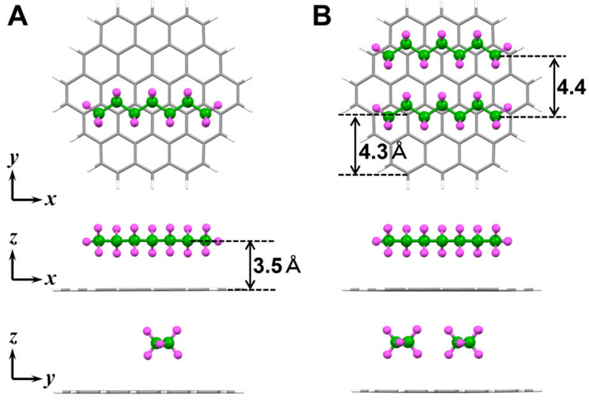

Fig. 1 Optimised geometries of *n*-heptane and an *n*-heptane dimer adsorbed on circumcoronene, as viewed from three directions. The carbon and hydrogen atoms of adsorbed *n*-heptane are coloured in green and pink, respectively.

The calculated E_{ad} of *n*-alkane is plotted as a function of *N*, as shown in Fig. 2(a). E_{ad} becomes larger (more negative) as *N* increases, and the linear increase in E_{ad} is consistent with the results of TPD reported by Tait et al.[2e] (Fig. S4) and previous theoretical studies.[9b,c] The increase in E_{ad} per CH_2 unit (ΔE_{ad}) is -1.85 kcal mol^{-1}, and this absolute value is almost identical to the experimental value (approximately 1.90 kcal mol^{-1}, Fig. S4). Therefore, our DFT calculations accurately evaluate the E_{ad}

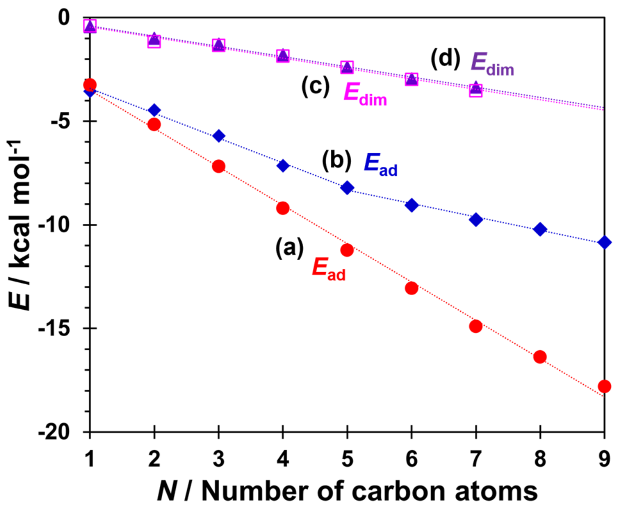

Fig. 2 Carbon number dependence of the adsorption energies (E_{ad}) of a single *n*-alkane and *n*-perfluoroalkane and the interaction energy between two adsorbed molecules (E_{dim}): (a) E_{ad} of *n*-alkane (red circles), $E_{ad} = -1.85N - 1.64$ ($R^2 = 0.997$); (b) E_{ad} of *n*-perfluoroalkane (blue rhombi), $E_{ad} = -1.20N - 2.22$ ($R^2 = 0.995$) for $N = 1$–5, $E_{ad} = -0.65N - 5.09$ ($R^2 = 0.989$) for $N = 5$–9; (c) E_{dim} of *n*-alkane (pink squares), $E_{dim} = -0.50N + 0.05$ ($R^2 = 0.989$); (d) E_{dim} of *n*-perfluoroalkane (purple triangles), $E_{dim} = -0.49N + 0.09$ ($R^2 = 0.994$). Numerical values are shown in Table S3.

values of *n*-alkanes on graphite. The interactions between the adsorbed *n*-alkanes and circumcoronene are significant, and the calculated E_{ad} of *n*-C_6H_{14} (-13.06 kcal mol^{-1}) is more than double the interaction energy of the hydrogen bond of a water dimer (approximately -5 kcal mol^{-1}).[22]

The E_{int} values obtained via the DFT calculations with and without the dispersion correction are shown in Fig. S5A. The E_{int} values obtained without the dispersion correction are positive, whereas those obtained using the dispersion correction are large negative values, indicating that the dispersion interactions are mainly responsible for stabilisation. The E_{int} between *n*-pentane and circumcoronene calculated using the optimised geometry, and contributions of the electrostatic (E_{es}), induction (E_{ind}), short-range (E_{es}), and dispersion (E_{disp}) interactions are shown in Table 1. The dispersion and short-range interactions (mainly exchange-repulsion) are the main contributors, and the dispersion interactions mainly induce attraction. The contributions of the electrostatic and induction interactions are small compared to those of the dispersion interactions. The details of the calculations of each energy component are shown in the ESI. The calculated interaction energy potential of the circumcoronene complex with *n*-pentane (Fig. 3) indicates that the equilibrium separation is determined by the balance between the exchange-repulsion and dispersion interactions.

Table 1 Calculated intermolecular interaction energies of complexes of *n*-pentane and *n*-perfluoropentane with circumcoronene, and the contributions of electrostatic, induction, short-range (orbital-orbital), and dispersion interactions.[a]

Complex	E_{int}[b]	E_{es}[c]	E_{ind}[d]	E_{short}[e]	E_{disp}[f]
n-pentane	–11.23	0.50	–0.05	4.64	–16.32
n-perfluoropentane	–8.84	–0.18	–0.06	4.09	–12.69

[a] Energy in kcal mol^{-1}. [b] Total interaction energy. [c] Electrostatic energy. [d] Induction energy. [e] Contributions of short-range (orbital-orbital) interactions ($E_{short} = E_{b3lyp} - E_{es} - E_{ind}$). E_{b3lyp} is the B3LYP/6-311G**-level interaction energy without dispersion correction. [f] Dispersion energy ($E_{disp} = E_{int} - E_{b3lyp}$).

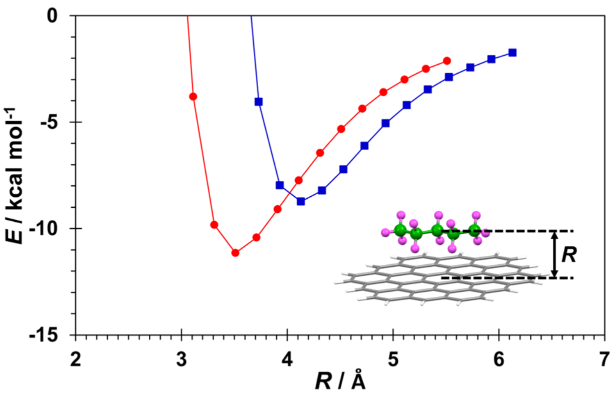

Fig. 3 Interaction energy (E_{int}) potentials of the *n*-pentane- (red circles) and *n*-perfluoropentane-circumcoronene complexes (blue rhombi). *n*-Pentane and *n*-perfluoropentane molecules were moved vertically from their optimised geometries, and *R* is the distance from the plane of circumcoronene.

In the optimised geometries, hydrogen atoms are located close to the centres of the six-membered rings of circumcoronene. These geometries are appropriate in reducing steric repulsion between the aromatic carbons and hydrogen atoms of the *n*-alkanes and decreasing the distance from circumcoronene. A short separation is advantageous in increasing stabilisation via the dispersion interactions.

To quantitatively evaluate the differences in the adsorption of *n*-alkanes and *n*-perfluoroalkanes, the geometries of adsorbed single *n*-perfluoroalkanes on circumcoronene were optimised and their E_{ad} values were calculated. The optimised geometries of the adsorbed *n*-perfluoroalkanes are shown in Figs. 4A and S8. In contrast to the stable helical conformations of isolated *n*-perfluoroalkanes (Fig. S9)[23], the optimised geometries of the adsorbed single *n*-perfluoroalkanes are almost planar (Fig. S8). The fluorine atoms of the *n*-

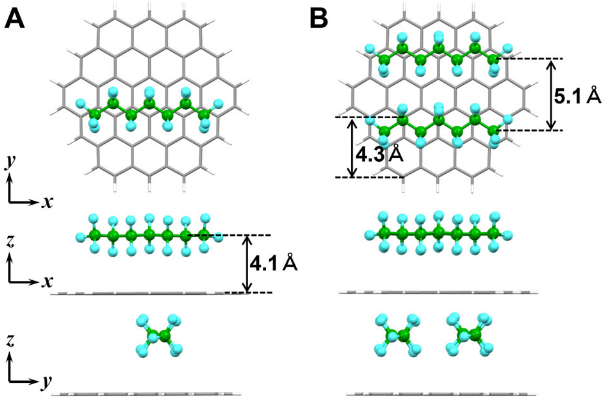

Fig. 4 Optimised geometries of *n*-perfluoroheptane and an *n*-perfluoroheptane dimer adsorbed on circumcoronene, as viewed from three directions. The carbon and fluorine atoms of adsorbed *n*-perfluoroheptane are coloured in green and cyan, respectively.

perfluoroalkanes are located close to the centres of the six-membered rings of circumcoronene, as in *n*-alkane adsorption. The distances between the carbon atoms of the adsorbed *n*-perfluoroalkanes and the π-plane are approximately 4.1 Å, which are higher than those of *n*-alkanes (3.5 Å). This is attributed to the larger steric repulsion of *n*-perfluoroalkanes.

The interactions of *n*-perfluoroalkanes with circumcoronene are weaker than those of the corresponding *n*-alkanes. The calculated E_{ad} values of *n*-perfluoroalkanes (Fig. 2(b)) are significantly smaller (less negative) than those of the corresponding *n*-alkanes, e.g. the E_{ad} values of *n*-C_6F_{14} and *n*-C_6H_{14} are -9.05 and -13.06 kcal mol^{-1}, respectively. The E_{int} values obtained via the DFT calculations with and without the dispersion correction are shown in Fig. S5B. The calculated E_{int} of the optimised geometry of the circumcoronene complex with *n*-perfluoropentane and the contributions of the energy terms are shown in Table 1. The dispersion interactions are mainly responsible for the attraction between an *n*-perfluoroalkane and circumcoronene, as in *n*-alkane adsorption. The calculated interaction energy potentials (E_{int}) of the circumcoronene complexes with *n*-pentane and *n*-perfluoropentane were compared, as shown in Fig. 3. The attraction in the *n*-perfluoropentane complex is stronger than that in the *n*-pentane complex when the vertical distances are large ($R \geq 4.1$ Å). Conversely, the calculated E_{int} of the *n*-pentane complex at the equilibrium distance (3.51 Å) is larger (more negative) than that of the *n*-perfluoropentane complex (4.13 Å) owing to the shorter intermolecular distance, which increases the stabilisation due to the dispersion interactions. Apparently, the shorter intermolecular distances in the stable structures of the *n*-alkane complexes compared to those of the *n*-perfluoroalkane complexes result in the higher stabilities of the adsorbed *n*-alkanes compared to those of the adsorbed *n*-perfluoroalkanes.

In contrast to the *n*-alkanes, the calculated E_{ad} values of the *n*-perfluoroalkane complexes do not increase linearly (Fig. 2(b)). The increase in E_{ad} per CF_2 unit (ΔE_{ad}) is -1.20 kcal mol^{-1} when $N = 1$–5 and -0.65 kcal mol^{-1} when $N = 5$–9. The E_{int} values of the *n*-perfluoroalkane complexes increase linearly within the entire range $N = 1$–9, as shown in Fig. S10D. Conversely, E_{def} is negligible when $N = 1$–5, whereas it increases as N increases when $N = 6$–9. Apparently, the large conformational changes associated with the adsorption of long *n*-perfluoroalkane chains (Figs. S9 and S10C) induce the increase in E_{def} when $N = 6$–9 (Fig. 2(b)). In contrast to the adsorption of *n*-perfluoroalkanes, the calculated E_{def} values of the adsorption of long *n*-alkanes are negligible (Fig. S10B), owing to the small conformational changes associated with adsorption (Fig. S10A). The calculated E_{int} values of *n*-perfluoroalkane complexes, which do not include the effects of conformation changes (E_{def}), are smaller (less negative) than those of *n*-alkane complexes owing to the longer intermolecular distances, as shown in Figs. S10B and S10D. The smaller E_{int} values of the *n*-perfluoroalkane complexes compared to those of the *n*-alkane complexes are the primary causes of the smaller E_{ad} values of *n*-perfluoroalkanes, while the larger E_{def} values of long *n*-perfluoroalkanes is also one of the factors that destabilise their adsorption.

The optimised geometries of adsorbed *n*-alkane dimers on circumcoronene are shown in Figs. 1B and S6. The intermolecular distances between the two adsorbed *n*-alkanes are approximately 4.4 Å, which are almost identical to the equilibrium distance of *n*-alkane dimers in the same configuration. These distances are also similar to the width of two units of six-membered rings in circumcoronene (4.3 Å, Fig. 1B). The interaction energies between the two adsorbed *n*-alkanes (E_{dim}) were then calculated without circumcoronene by changing the intermolecular distances (Fig. S7). The calculated E_{dim} values of C_3H_8, C_5H_{12}, and C_7H_{16} exhibit minima at ~4.4 Å. The E_{dim} plotted as a function of N (Fig. 2(c)) indicates that the increase in E_{dim} per CH_2 unit (ΔE_{dim}) is -0.50 kcal mol^{-1}. Although ΔE_{ad} is more than three-fold larger than ΔE_{dim}, the contributions of the interactions between adsorbed *n*-alkane molecules in stabilisation are not negligible.

The optimised geometries of the *n*-perfluoroalkane dimers adsorbed on circumcoronene are shown in Figs. 4B and S11. The distances between the corresponding carbon atoms of the two adsorbed molecules are ~5.1 Å. The interaction energies between the two adsorbed *n*-perfluoroalkanes (E_{dim}) were also calculated by changing the intermolecular distances (Fig. S7). These distances between two *n*-perfluoroalkanes in the optimised geometries are slightly smaller than the equilibrium distances (~5.3 Å), although the differences in their E_{dim} values are almost negligible (≤0.1 kcal mol^{-1}). E_{dim} was plotted as a function of N of a *n*-perfluoroalkane, as shown in Fig. 2(d). The E_{dim} values of *n*-perfluoroalkanes are similar to those of the corresponding *n*-alkanes, e.g. the E_{dim} values of *n*-C_6F_{14} and *n*-C_6H_{14} are -2.96 and -2.98 kcal mol^{-1}, respectively. The increase in E_{dim} per CF_2 unit (ΔE_{dim}) is -0.49 kcal mol^{-1}, which is almost identical to the ΔE_{dim} of an *n*-alkane.

The intermolecular distances between the *n*-perfluoroalkanes in the adsorbed dimers (~5.1 Å) are longer than the width of two units of six-membered rings in circumcoronene (4.3 Å). The positions of the *n*-perfluoroalkanes in the optimised geometries of the adsorbed dimers (the position of the molecule close to the centre of circumcoronene, Fig. 4B) differ from those in the optimised geometries of adsorbed single molecules (Fig. 4A) owing to the lattice mismatch, which destabilises the adsorbed *n*-perfluoroalkane dimers (Fig. S11), e.g. the calculated E_{ad} of one *n*-C_6F_{14} using the optimised geometry of the adsorbed dimer (-8.06 kcal mol^{-1}) is smaller (less negative) than that calculated using the optimised geometry of the adsorbed single molecule (-9.05 kcal mol^{-1}). The higher N is, the larger the decrease in E_{ad} owing to the mismatch. Therefore, close-packed adsorbed *n*-perfluoroalkanes on circumcoronene sacrifice E_{ad} to maintain the larger equilibrium intermolecular distances between the *n*-perfluoroalkanes.

Adsorbed structures of *n*-C_6H_{14} and *n*-C_6F_{14} in another arrangement (edge-on) were optimised. The initial structures used in the geometry optimisations were prepared by rotating the flat-on adsorbed molecules by approximately 90˚ around the long axes of the molecules. The calculated E_{ad} values of the

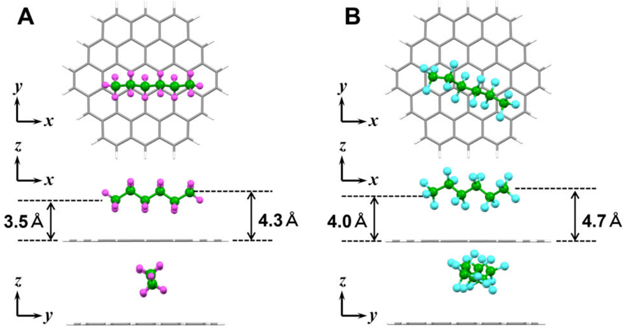

Fig. 5 Optimised geometries of edge-on oriented (A) *n*-C_6H_{14} and (B) *n*-C_6F_{14} on circumcoronene, as viewed from three directions. The carbon, hydrogen and fluorine atoms of adsorbed molecules are coloured in green, pink and cyan, respectively.

optimised structures of edge-on adsorbed *n*-C_6H_{14} and *n*-C_6F_{14} (Fig. 5) are –10.35 and –8.41 kcal mol^{-1}, respectively, which are smaller (less negative) than those of the optimised flat-on adsorbed structures. Therefore, the flat-on structures are more stable than the edge-on structures. The calculated E_{ad} of the edge-on adsorbed *n*-C_6H_{14} is 2.72 kcal mol^{-1} smaller than that of the flat-on adsorbed *n*-C_6H_{14}, whereas the difference in the calculated E_{ad} values of the edge-on and flat-on adsorbed *n*-C_6F_{14} is only –0.63 kcal mol^{-1}. This suggests that the energy change of adsorbed *n*-perfluoroalkane associated with the rotation is smaller than that of corresponding *n*-alkane.

Conclusions

The E_{ad} values of *n*-alkanes and *n*-perfluoroalkanes on circumcoronene were evaluated using dispersion-corrected DFT calculations. The adsorbed *n*-perfluoroalkanes were flat, in contrast to the stable helical structures of isolated *n*-perfluoroalkanes. The *n*-perfluoroalkanes displayed smaller (less negative) E_{ad} values compared to those of the corresponding *n*-alkanes. The dispersion interactions were the major source of the attraction between adsorbed molecules (*n*-alkanes and *n*-perfluoroalkanes) and circumcoronene. The larger steric repulsion of *n*-perfluoroalkanes compared to those of *n*-alkanes, which increased the equilibrium distance from circumcoronene and decreased the dispersion interactions, caused the smaller E_{ad} values of *n*-perfluoroalkanes compared to those of *n*-alkanes.

Although the interactions between adsorbed molecules were weaker than those of adsorbed molecules with circumcoronene, the contributions of the interactions between adsorbed molecules in their stabilisation were not negligible. The equilibrium distances between two adsorbed *n*-alkanes were similar to the width of two six-membered rings in circumcoronene, whereas the equilibrium distances between two adsorbed *n*-perfluoroalkanes were larger, and thus, lattice mismatch occurred, which destabilised the adsorbed *n*-perfluoroalkanes. The difference in the E_{ad} values between flat-on and edge-on orientations of *n*-C_6F_{14} was smaller than that of *n*-C_6F_{14}, suggesting that the energy change of adsorbed *n*-perfluoroalkane associated with the rotation is smaller than that of corresponding *n*-alkane. These results explain the experimentally observed preferential adsorption of *n*-alkanes on graphite over *n*-perfluoroalkanes. Thus, we elucidated the origin of the attraction between adsorbed molecules (*n*-alkanes and *n*-perfluoroalkanes) and circumcoronene, and explained the higher stabilities of adsorbed *n*-alkanes compared to those of adsorbed *n*-perfluoroalkanes.

This study enhances our understanding of supramolecular chemistry on surfaces, and can also prove useful in the molecular design of building blocks that assemble into well-ordered nanostructures for use in practical applications, such as molecular devices and circuits. Quantitative studies based on DFT calculations for plausible parts of the building blocks are currently underway.

Conflicts of interest

There are no conflicts to declare.

Acknowledgements

This work was partially supported by A-STEP (JPMJTR20U3 to Y.K.) and CREST (JPMJCR18J2 to S.T.) from the Japan Science and Technology Agency.

Notes and references

1 (a) M. Kind and C. Wöll, *Prog. Surf. Sci.*, 2009, **84**, 230–278. (b) D. B. Amabilino, *Supramolecular Chemistry at Surfaces*, Royal Society of Chemistry, London, 2016. (c) Y. Meng, J. Xu, L. Ma, Z. Jin, B. Prakash, T. Ma and W. Wang, *Friction*, 2022, **10**, 1443–1595.

2 (a) K. R. Paserba and A. J. Gellman, *Phys. Rev. Lett.*, 2001, **86**, 4338–4341. (b) K. R. Paserba and A. J. Gellman, *J. Chem. Phys.*, 2001, **115**, 6737–6751. (c) A. J. Gellman and K. R. Paserba, *J. Phys. Chem. B*, 2002, **106**, 13231–13241. (d) R. Zacharia, H. Ulbricht and T. Hertel, *Phys. Rev. B,* 2004, **69**, 155406. (e) H. Ulbricht, R. Zacharia, N. Cindir and T. Hertel, *Carbon*, 2006, **44**, 2931–2942. (e) S. L. Tait, Z. Dohnálek, C.T. Campbell and B. D. Kay, *J. Chem. Phys.*, 2006, **125**, 234308.

3 (a) J. V. Barth, G. Costantini and K. Kern, *Nature*, 2005, **437**, 671–679. (b) E. Gomar-Nadal, J. Puigmartí-Luis and D. B. Amabilino, *Chem. Soc. Rev*., 2008, **37**, 490–504. (c) C. Tang, E. M. Lennon, G. H. Fredrickson, E. J. Kramer and C. J. Hawker, *Science,* 2008, **322**, 429–432. (d) D. B. Amabilino, *Supramolecular Chemistry at Surfaces*, Royal Society of Chemistry, Cambridge, 2016. (e) M. Gobbi, S. Bonacchi, J. X. Lian, Y. Liu, X.-Y. Wang, M.-A. Stoeckel, M. A. Squillaci, G. D'Avino, A. Narita, K. Müllen, X. Feng, Y. Olivier, D. Beljonne, P. Samorì and E. Orgiu, *Nat. Commun*., 2017, **8**, 14767. (f) S. A. Claridge, *Chem. Commun.*, 2018, **54**, 6681–6691.

4 (a) K. S. Mali, J. Adisoejoso, E. Ghijsens, I. De Cat and S. De Feyter, *Acc. Chem. Res.*, 2012, **45**, 1309–1320. (b) N. Nishitani, T. Hirose and K. Matsuda, *Langmuir*, 2017, **33**, 9151–9159. (c) Y. Wu, J. Li, Y. Yuan, M. Dong, B. Zha, X. Miao, Y. Hu and W. Deng, *Phys. Chem. Chem. Phys.*, 2017, **19**, 3143–3150. (d) J. Li, B. Tu, X. Li, C. Ma, C. Chen, W. Duan, X. Xiao and Q. Zeng, *Chem. Commun*., 2019, **55**, 11599–11602. (e) O. Ochs, M. Hocke, S. Spitzer, W. M. Heckl, N. Martsinovich and M. Lackinger, *Chem. Mater.*, 2020, **32**, 5057–5065. (f) G. Velpula, C. Martin, B. Daelemans, G. Hennrich, M. Van der Auweraer, K. S. Mali and S. De Feyter, *Chem. Sci.*, 2021, **12**, 13167–13176.

5 (a) Y.-F. Geng, P. Li, J.-Z. Li, X.-M. Zhang, Q.-D. Zeng and C. Wang, *Coord. Chem. Rev.*, 2017, **337**, 145–177. (b) M.-A. Carvalho, H. Dekkiche, M. Nagasaki, Y. Kikkawa and R. Ruppert, *J. Am. Chem. Soc.*, 2019, **141**, 10137–10141. (c) X. Sun, X. Yao, F. Lafolet, G. Lemercier and J.-C. Lacroix, *J. Phys. Chem. Lett.*, 2019, **10**, 4164–4169. (d) Y. Kikkawa, M. Nagasaki, S. Tsuzuki, T. N. J. Fouquet, S. Nakamura, Y. Takenaka, Y. Norikane and K. Hiratani, *Chem. Commun.*, 2022, **58**, 1752–1755.

6 (a) Q.-N. Zheng, X.-H. Liu, T. Chen, H.-J. Yan, T. Cook, D. Wang, P. J. Stang and L.-J. Wan, *J. Am. Chem. Soc.*, 2015, **137**, 6128–6131. (b) A. Mukherjee, J. Teyssandier, G. Hennrich, S. De Feyter and K. S. Mali, *Chem. Sci.*, 2017, **8**, 3759–3769. (c) Z. Guo, P. Yu, K. Sun, S. Lei, Y. Yi and Z. Li, *Phys. Chem. Chem. Phys.*, 2017, **19**, 31540–31544. (d) F. Silly, *J. Phys. Chem. C*, 2017, **121**, 10413–10418. (e) Y. Kikkawa, M. Nagasaki, E. Koyama, S. Tsuzuki and K. Hiratani, *Chem. Commun.*, 2019, **55**, 3955–3958. (f) Y. Kikkawa, M. Nagasaki, E. Koyama, S. Tsuzuki, T. Fouquet and K. Hiratani, *Nanoscale Adv*., 2020, **2**, 4895–4901. (g) Y. Kikkawa, M. Nagasaki, E. Koyama, S. Ito and S. Tsuzuki, *Phys. Chem. Chem. Phys.*, 2022, **24**, 17088–17097.

7 (a) F. Tao and S. L. Bernasek, *Chem. Rev.*, 2007, **107**, 1408–1453. (b) Y. Kikkawa, E. Koyama, S. Tsuzuki, K. Fujiwara and M. Kanesato, *Langmuir*, 2010, **26**, 3376–3381. (c) Y. Hu, K. Miao, L. Xu, B. Zha, X. Miao and W. Deng, *RSC Adv.,* 2017, **7**, 32391–32398. (d) Y. Fang, M. Cibian, G. S. Hanan, D. F. Perepichka, S. De Feyter, L. A. Cuccia and O. Ivasenko, *Nanoscale*, 2018, **10**, 14993–15002. (e) M. Maeda, R. Nakayama, S. De Feyter, Y. Tobe and K. Tahara, *Chem. Sci.*, 2020, **11**, 9254–9261.

8 (a) R. Hentschke, B. L. Schürmann and J. P. Rabe, *J. Chem. Phys.*, 1992, **96**, 6213–6221. (b) S. Yin, C. Wang, X. Qiu, B. Xu and C. Bai, *Surf. Int. Anal.*, 2001, **32**, 248–252. (c) T. Yang, S. Berber, J.-F. Liu, G. P. Miller and D. Tománek, *J. Chem. Phys.*, 2008, **128**, 124709. (d) B. Ilan, G. M. Florio, M. S. Hybertsen, B. J. Berne and G. W. Flynn, *Nano Lett.*, 2008, **8**, 3160–3165. (e) L. Verstraete, T. Rinkovec, H. Cao, H. I. Reeves, J. N. Harvey and S. De Feyter, *J. Phys. Chem. C,* 2021, **125**, 1557–1563.

9 (a) C. Thierfelder, M. Witte, S. Blankenburg, E. Rauls and W. G. Schmidt, *Surf. Sci.,* 2011, **605**, 746–749. (b) E. Londero, E. K. Karlson, M. Landahl, D. Ostrovskii, J. D. Rydberg and E. Schröder, *J. Phys. Condens. Matter,* 2012*,* **24**, 424212. (c) K. Kamiya and S. Okada, *Jpn. J. Appl. Phys.* 2013, **52**, 04CN07.

10 (a) C. M. Mate, *Tribol. Lett.*, 1998, **4**, 119−123. (b) A. J. Gellman, *Curr. Opin. Colloid Interface Sci.* 1998, **3**, 368−372. (c) G. W. Tyndall and R. J. Waltman, *J. Phys. Chem. B*, 2000, **104**, 7085−7095. (d) A. Khurshudov and R. J. Waltman, *Tribol. Lett.*, 2001, **11**, 143−149.

11 (a) A. Stabel, L. Dasaradhi, D. O’Hagan and J. P. Rabe, *Langmuir*, 1995, **11**, 1427–1430. (b) C. L. Claypool, F. Faglioni, W. A. Goddard, H. B. Gray, N. S. Lewis and R. A. Marcus, *J. Phys. Chem. B*, 1997, **101**, 5978–5995. (c) R. Lazzaroni, A. Calderone, J. L. Brédas and J. P. Rabe, *J. Chem. Phys.* 1997, **107**, 99–105. (c) A. Gesquière, M. M. Abdel-Mottaleb, F. C. De Schryver, M. Sieffert and K. Müllen, *Langmuir*, 1999, **15**, 20, 6821–6824. (d) M. M. S. Abdel-Mottaleb, S. De Feyter, M. Sieffert, M. Klapper, K. Müllen and F. C. De Schryver, *Langmuir*, 2003, **19**, 8256–8261. (e) A. Gesquière, M. M. Abdel-Mottaleb, S. De Feyter, F. C. De Schryver, M. Sieffert, K. Müllen, A. Calderone, R. Lazzaroni and J.-L. Brédas, *Chem. Eur. J.*, 2000, **6**, 3739–3746. (f) Y. Kikkawa, S. Tsuzuki, K. Taguchi, A. Kashiwada and K. Hiratani, *Phys. Chem. Chem. Phys.*, 2017, **19**, 13579–13584.

12 J. E. Parker, S. M. Clarke and A. C. Perdigón, *Surf. Sci.*, 2007, **601**, 4149–4153.

13 S. Conti and M. Cecchini, *J. Phys. Chem. C*, 2015, **119**, 1867–1879.

14 J. A. Pople, M. Head-Gordon, K. Raghavachari, *J. Chem. Phys.* 1987, **87**, 5968.

15 T. H. Dunning Jr., *J. Phys. Chem. A*, 2000, **104**, 9062–9080.

16 Seiji Tsuzuki and Tadafumi Uchimaru, *Phys. Chem. Chem. Phys.*, 2020, **22**, 22508–22519.

17 M. J. Frisch, G. W. Trucks, H. B. Schlegel, G. E. Scuseria, M. A. Robb, J. R. Cheeseman, G. Scalmani, V. Barone, G. A. Petersson, H. Nakatsuji, X. Li, M. Caricato, A. V. Marenich, J. Bloino, B. G. Janesko, R. Gomperts, B. Mennucci, H. P. Hratchian, J. V. Ortiz, A. F. Izmaylov, J. L. Sonnenberg, D. Williams-Young, F. Ding, F. Lipparini, F. Egidi, J. Goings, B. Peng, A. Petrone, T. Henderson, D. Ranasinghe, V. G. Zakrzewski, J. Gao, N. Rega, G. Zheng, W. Liang, M. Hada, M. Ehara, K. Toyota, R. Fukuda, J. Hasegawa, M. Ishida, T. Nakajima, Y. Honda, O. Kitao, H. Nakai, T. Vreven, K. Throssell, J. A. Montgomery, Jr., J. E. Peralta, F. Ogliaro, M. J. Bearpark, J. J. Heyd, E. N. Brothers, K. N. Kudin, V. N. Staroverov, T. A. Keith, R. Kobayashi, J. Normand, K. Raghavachari, A. P. Rendell, J. C. Burant, S. S. Iyengar, J. Tomasi, M. Cossi, J. M. Millam, M. Klene, C. Adamo, R. Cammi, J. W. Ochterski, R. L. Martin, K. Morokuma, O. Farkas, J. B. Foresman and D. J. Fox, Gaussian 16, Revision C.01, Gaussian, Inc., Wallingford, CT, 2016.

18 A. D. Becke, *J. Chem. Phys*., 1993, **98**, 5648–5652.

19 S. Grimme, J. Antony, S. Ehrlich and H. Krieg, *J. Chem. Phys*., 2010, **132**, 154104.

20 B. J. Ransil, *J. Chem. Phys*., 1961, **34**, 2109–2118.

21 S. F. Boys and F. Bernardi, *Mol. Phys.*, 1970, **19**, 553–566.

22 S. Tsuzuki, A. Wakisaka, T. Ono and T. Sonoda, *Chem. Eur. J.* 2012, **18**, 951–960.

23 (a) C. W. Bunn and E. R. Howells, *Nature*, 1954, **174**, 549–551. (b) E. K. Watkins and W. L. Jorgensen, *J. Phys. Chem. A*, 2001, **105**, 4118–4125. (c) S. S. Jang, M. Blanco, W. A. Goddard, G. Caldwell and R. B. Ross, *Macromolecules*, 2003, **36**, 5331–5341. (d) R. A. Cormanich, D. O’Hagen and M. Bühl, *Angew. Chem. Int. Ed. Engl.,* 2017, **56**, 7867–7870.